ACS APPLIED MATERIALS & INTERFACES

Research Article

www.acsami.org

Asymmetric Plasmonic Aptasensor for Sensitive Detection of Bisphenol A

Hua Kuang,*,† Honghong Yin,† Liqiang Liu, Liguang Xu, Wei Ma, and Chuanlai Xu

State Key Lab of Food Science and Technology, School of Food Science and Technology, Jiangnan University, Wuxi, Jiangsu 214122, China

Supporting Information

ABSTRACT: A sensitive plasmonic chirality-based aptasensor for the detection of bisphenol A (BPA) was developed. Asymmetric plasmonic nanoparticle dimers were produced by the hybridization of a BPA aptamer and its complementary sequence modified nanoparticles. Under different concentrations of BPA, the intensity of the chiral signal was varied. A low limit of detection of 0.008 ng/mL was obtained in the range 0.02−5 ng/mL.

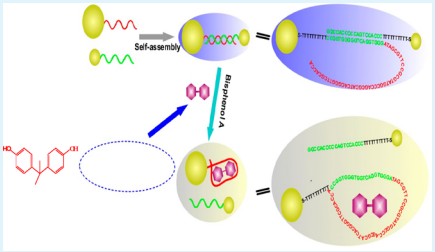

KEYWORDS: *sensitive, asymmetric, plasmonic, aptasensor, bisphenol A, detection*

1. INTRODUCTION

Bisphenol A (BPA) is an important organic chemical and is widely used in the production of epoxy resins, polycarbonate plastics, flame retardants, and dental sealants. Thus, BPA is ubiquitous in the lacquers coating metal products, food and drink packaging such as food cans, nursing bottles, beverage containers, and in water supply pipes. As BPA rapidly enters the environment and the food chain, widespread human exposure to significant doses of this compound has been discovered.[1−5] A number of studies have indicated that BPA is an environmental endocrine disrupting chemical (EDC) with potential estrogenic activity. It acts on endogenous hormones, both estrogens and androgens, to disrupt normal endocrine function, influencing sexual development and reproduction in both male and female humans and animals. In addition, various types of cancers and diverse pleiotropic actions in the brain and cardiovascular system are related to the intake of BPA.[6−8]

Conventional techniques used in the quantification of BPA are mainly focused on instrument-based methods, such as high pressure liquid chromatography (HPLC), liquid chromatography (LC), liquid chromatography coupled with mass spectrometry (LC−MS), gas chromatography (GC), and gas chromatography coupled with mass spectrometry (GC−MS).[9−12] It has been reported that the limit of detection (LOD) of BPA analyzed using these methods could reach an ideal level. However, expensive instruments, complicated and time-consuming sample preparation steps, and skilled operators are required, which restricts their wide application. Enzyme-linked immunosorbent assay (ELISA), which is a convenient and inexpensive technique, has also been used in the detection of BPA. This method is strongly dependent on the antibody recognizing the target, which has been challenging due to the stability of the antibody and nonspecific binding to BPA analogs.[13,14]

Aptamers are a new type of single-stranded DNA or RNA nucleic acid recognition probe, which have been widely used in the detection of numerous targets instead of antibodies.[15−20] The advantages of aptamers, which include thermal stability, reusability, and easy manufacture, make them comparable to antibodies. Since the BPA aptamer was first screened in 2011, many related papers on the use of aptamers in the detection of BPA have been reported.[21−26] Therefore, in our work, BPA aptamers were utilized as replacement probes for antibodies in the detection of BPA.

Nanomaterials possess specific properties, such as optical, electrochemical, fluorescent, piezoelectric, and magnetic, which have attracted wide attention and a considerable amount of research has been carried out on nanostructural characteristics and detection sensors.[27−29] With the increasing development of nanotechnology, the chirality of nanomaterial assemblies has received more attention. Circular dichroism (CD) originating from the chiral structures assembled by plasmonic nanoparticles can be measured.[30−32] Alivisatos' group built chiral enantiomers using four different sized gold nanoparticles (Au NPs) and proposed the concept of the chiral plasmonic nanostructures of Au NPs with tetrahedral symmetry.[33] Gold nanorods assembly driven by DNA hybridization also produced obvious plasmonic CD signals.[34,35]

Various Au NPs nanostructures including dimers, trimers, tetramers, and complex agglomerates also have chiral optical activity, and the CD signal of the dimer is higher than that of the other structures. Importantly, strong CD can be used as a detection signal for constructing sensors.[36−39] The CD signal produced by the Au NPs dimers assembled through immuno-

Received: October 7, 2013
Accepted: November 19, 2013
Published: November 19, 2013

Scheme 1. Scheme of BPA Detection Based on Asymmetric Plasmonic Dimer

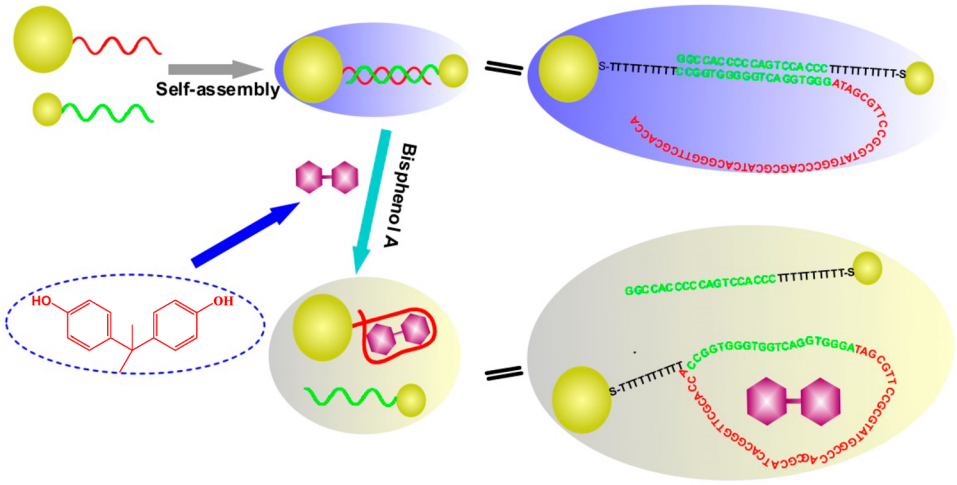

recognition has been researched by our group in the detection of BPA, and the LOD was 0.02 ng/mL.[40] However, the limited recognition ability of antibody/antigen toward various analytes and loss of their recognized activity upon binding on nanoparticles (e.g., the recognition site of antibodies may modify on the surface of nanoparticles) make these recognizing units unsuitable for the design of high stability sensors.

Herein, we developed a more selective and sensitive chirality-based aptamer sensor for BPA detection, as illustrated in Scheme 1. An anti-BPA aptamer and its complementary fragment, respectively modified by 20 and 10 nm Au NPs, were assembled into asymmetric dimers by DNA-induced hybridization. As it was reported that the dissociation constants (K_d) of the BPA was 8.3nM[21] and the affinity of aptamer targeting BPA is comparable to that of a high-affinity antibody (3−10nM).

In the presence of BPA, the anti-BPA aptamer prefers to switch its configuration to combine with the BPA target, resulting in the release of complementary oligonucleotide. Correspondingly, the Au NPs dimers were disaggregated into dispersed nanoparticles. The CD intensity of the reaction system correlated with the number of dimers. Therefore, the higher the concentration of the BPA target, the less the number of Au NPs dimers and the weaker the CD intensity of the sensor.

2. EXPERIMENTAL SECTION

2.1. Synthesis of Gold Nanoparticles. Au NPs with a diameter of 20 and 10 nm were all synthesized by reduction of $HAuCl_4$ using trisodium citrate. For 10 nm Au NPs, briefly, 2.0 mL of aqueous trisodium citrate solution (1% by weight, freshly prepared) was quickly added to 100 mL of 0.25 mM boiling aqueous solution of $HAuCl_4$ under vigorous stirring and reflux. After several minutes, the color of the solution changed from blue to wine red. After the solution was boiled for another 15−30 min, the heat source was removed to allow for the reaction solution to cool to room temperature. The 10 nm Au NPs were then obtained. For 20 nm Au NPs, the added aqueous trisodium citrate solution (1% by weight, freshly prepared) was 1.2 mL, and other steps were the same with 10 nm Au NPs synthesized procedures.

The concentration of two kinds of newly synthesized Au NPs suspended in aqueous solutions was calculated according to the elemental gold content determined by inductively coupled plasma mass spectroscopy (ICP-MS) method.[41] And then the concentration of 10 and 20 nm Au NPs in the aqueous solutions were calculated as

$$c = \frac{m_1}{m_s \times N_A} \quad (1)$$

where m_1 is the gold content in the aqueous solutions as determined by ICP-MS, m_s is the average weight of one NP for 10 and 20 nm Au NPs, and N_A is 6.023×10^{23}. Hence, the concentration of 10 and 20 nm Au NPs was calculated as 4 and 1 nM, respectively.

2.2. Modification of 10 and 20 nm Au NPs. The DNA modification of Au NPs was conducted according to the previously published reports.[42] Briefly, the two kinds of newly synthesized Au NPs were all concentrated five times, and the final concentrations of 10 and 20 nm Au NPs were, respectively, 20 and 5 nM in 0.01 M phosphate buffer with 0.01% sodium dodecylsulfate (SDS). Ten nanometer Au NP−DNA_1 probes were prepared by derivatizing 50 μL of an aqueous 10 nm diameter Au NPs solution (20 nM) with 1 OD of fresh dissolved alkanethiol derivative of DNA_1 with 0.01 M phosphate buffer (containing 0.01% SDS) solution (final DNA_1 concentration is 100 μM). The coupling ratio of DNA_1 to 10 nm Au NPs was 5:1. The solution of DNA_1 and 10 nm Au NP was incubated for 20 min at room temperature. The concentration of NaCl was increased to 25 mM using 2 M NaCl and 0.01 M pH 8.0 phosphate buffer (containing 0.01% SDS). After a 20 min incubation period at room temperature, the solution of DNA_1 and 10 nm Au NP was then sonicated for 10 s. And this process was repeated one time to reach a concentration of 50 mM NaCl in the solution with 2 M NaCl and 0.01 M pH 8.0 phosphate buffer (containing 0.01% SDS). Hereafter, the reacted systems were followed by incubation about 12 h at room temperature. To remove the excess of DNA_1, Au NPs were centrifuged, and the supernatant was removed, leaving a pellet of Au NPs at the bottom. And then, the Au NPs were resuspended in 0.001 M Tris−HCl buffer (0.01% SDS, pH 8.0). This washing process was repeated for three times. Regarding for 20 nm Au NPs−DNA_2 conjugation, the process was similar to the synthesized procedure of 10 nm Au NPs−DNA_1. The coupling ratio of DNA_2 to 20 nm Au NPs was also 5:1. The DNA density on the nanoparticle surface was measured by a fluorescence-based method.[43] Detailed procedures of these methods are shown in the Supporting Information.

2.3. Assembly of Asymmetric Au NPs Dimers. First, 10 μL of 10 nm Au NP−DNA_1 was mixed with 40 μL of 20 nm Au NP−DNA_2 solution in 50 μL of 0.02 M Tris−HCl buffer (0.01% SDS, $MgCl_2$ 20 mM, KCl 40 mM, NaCl 100 mM, pH 8.0) with gentle shaking for 5 min. Six BPA standards, 0, 0.05, 0.1, 0.5, 1, and 5 ng/mL, were reconstituted with Millipore water (resistance > 18 MΩ/cm). To samples of the mixed solution, 100 μL of BPA standard solution with different concentrations were separately added and mixed well. The solution was then incubated for about 8 h at room temperature to form the asymmetric Au NPs dimers. After incubation, the sample was analyzed by Transmission electron microscopy (TEM), UV/vis, dynamic light scattering (DLS), and CD. A standard curve was

dx.doi.org/10.1021/am4043678 | ACS Appl. Mater. Interfaces 2014, 6, 364−369

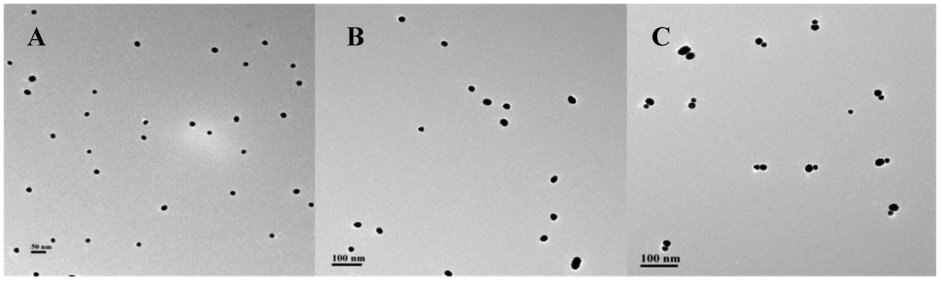

Figure 1. Representative TEM images of Au NPs: (A) the dispersed 10 nm Au NPs probes, (B) the dispersed 20 nm Au NPs probes, and (C) asymmetric Au NPs assembled dimers.

established by plotting the CD signal intensity against the concentration.

2.4. Instruments and Methods. Transmission electron microscopy (TEM) images were obtained using a JEOL 2100 microscope. The chirality of asymmetric Au NPs dimers was measured by MOS-450/AF-CD (Biologic). The size distribution of the asymmetric Au NPs dimers was measured by a dynamic light scattering instrument (Malvern Zetasizer Nano). The surface plasmon resonance spectra of the Au NPs and the reaction systems were measured by Biomate 3S UV−visible spectrophotometer (Thermo Electron).

3. RESULTS AND DISCUSSION

The 10 and 20 nm Au NPs were synthesized by reduction of $HAuCl_4$. The dispersibility and morphology of the two types of Au NPs were characterized by transmission electron microscopy (TEM) (Figure 1 A,B). The sulfhydryl-modified aptamer sequence was 5′-SH-$(T)_{10}$-CCGGT GGGTG GTCAG GTGGG ATAGC GTTCC GCGTA TGGCC CAGCG CATCA CGGGT TCGCA CCA-3′ (denoted DNA_2), and the complementary sequence was 5′-SH-$(T)_{10}$-CCCAC CTGAC CACCC ACCGG-3′ (denoted DNA_1).

The coupling ratio of the anti-BPA aptamer to 20 nm Au NPs was 5:1 and so was the complementary DNA fragment and 10 nm Au NPs ratio. According to the fluorescence methods,[43] the number of thiol-modified DNA_1 and DNA_2 molecules attached to each 10 and 20 nm nanoparticle was calculated to be 1.03 ± 0.03 and 1.14 ± 0.07, respectively (Figure S1, Supporting Information). Without the BPA target, the quality of the Au NPs asymmetric dimers assembled by the hybridization of DNA_1 and DNA_2 was assessed by transmission electron microscopy (TEM). Statistical analysis of 146 images for each of the nanoparticle assemblies revealed that the yields for NP dimers were as high as 72.2% (Figure 1C and S3 (Supporting Information)). The size distribution of the formed Au NPs dimers was measured by dynamic light scattering (DLS) (Figure 2). DLS is the most sensitive to the largest measure of the scattering particles. By taking into account the TEM diameter of 10 and 20 nm NPs modified with DNA as well as their DLS diameters equal to 22 and 40 nm with relatively narrow distribution (polydispersity index (PDI) = 0.292 and 0.281), respectively, the distance of DNA_1 (30 bp) and DNA_2 (73 bp) modified on the 10 and 20 nm NP can be estimated to be 12 ± 4 and 20 ± 3 nm. It should be noted that the length/base number in DNA_2 was shorter than that in DNA_1. Because of the high content of guanine in DNA_2 (%G in DNA_2 up to 31.5%), G-rich DNA_2 easily formed quadruplex structures and caused a hydrodiameter of DNA_2 shorter than that for DNA_1 modified onto the surface of NPs, respectively.[44]

In comparison with the 10 and 20 nm Au NPs−DNA probes, the hydrodynamic size of the assembled dimers showed an obvious increase. The increment in the hydrodynamic size also

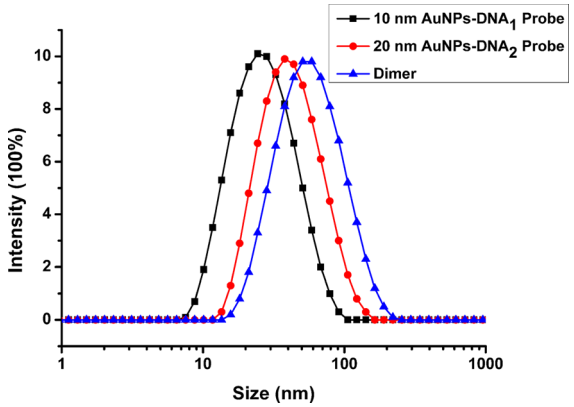

Figure 2. Hydrodynamic diameters of 10 and 20 nm Au NPs probes and asymmetric Au NPs dimers.

demonstrated that the asymmetric dimers were effectively produced.

Under optimized conditions, the sensitivity of this plasmonic chirality-based sensor was estimated by CD signals at different concentrations of BPA standard substance. The concentrations of BPA were 5, 1, 0.5, 0.1, 0.05, and 0.02 ng/mL, and the corresponding CD intensities are shown in Figure 3A. With increased BPA concentration, the CD intensity at 533 nm decreased with a reduction in the number of dimers. However, the UV/vis signal at 533 nm was almost the same (Figure 4). It was ascribed that the chiral absorption bands of the samples were always located at the visible region. Furthermore, our experimental results of Au NPs asymmetric dimers with 20 bp DNA bridges for the plasmon rulers, exhibiting the slight red shift compared to the individual NP probes, have been in good agreement with those of published results in the peak wavelength tendency of UV/vis spectra.[45−47] The standard curve of BPA detection was obtained by the CD values at 533 nm at the above concentrations of BPA. In the linear range 5−0.02 ng/mL, an excellent correlation of R^2 = 0.9940 was obtained and the LOD was 0.008 ng/mL. As shown in Table 1, this developed method has the merit of a much lower LOD compared to other detected methods for BPA except the fluorescence detection method.[48−52] Furthermore, scientific opinion on biosensors based on fluorescence techniques,[53−55] which typically contain a complex mixture of biological macromolecules (and lots of macromolecules have the fluorescence), will be challenging because of interference and poor specificity due to ubiquitous nonspecific interactions and background fluorescence interference.

To confirm the specificity and selectively of this method, three types of BPA analogs Bisphenol C (BPC), Biphenolic

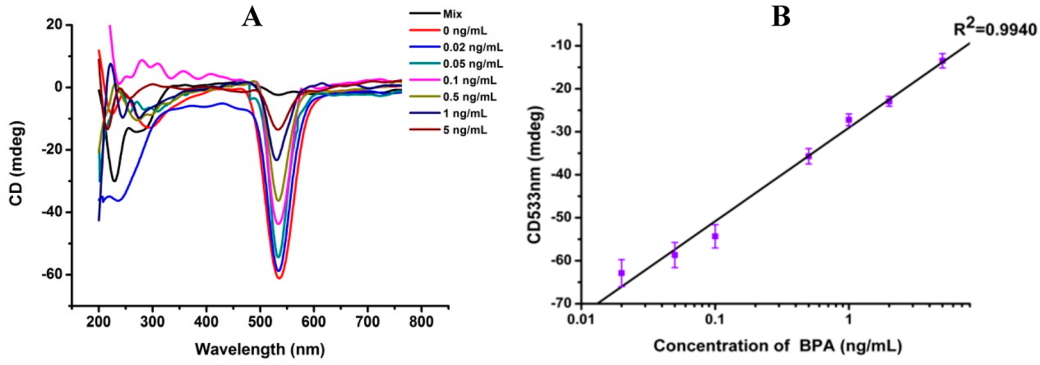

Figure 3. (A) CD spectral under different concentrations of BPA, and the concentrations of BPA were 5, 1, 0.5, 0.1, 0.05, and 0.02 ng/mL. (B) Standard curve of the determination of target BPA.

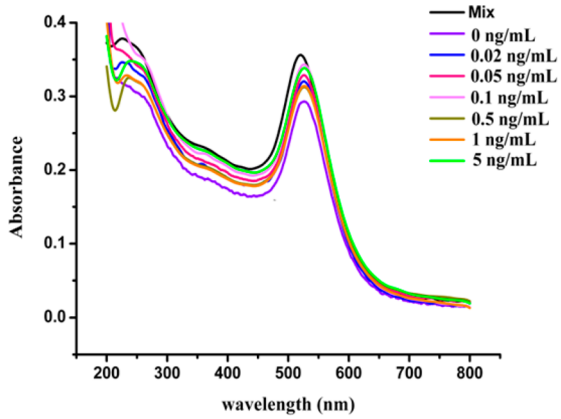

Figure 4. UV/vis spectra of the reaction system under different concentrations of BPA.

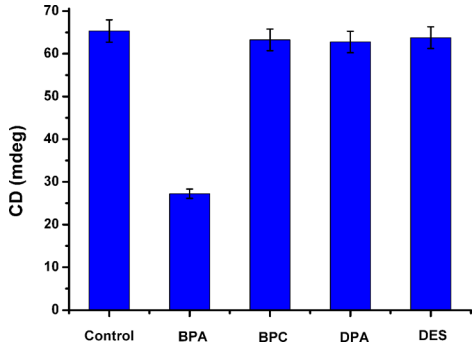

Figure 5. CD spectral change of the detection of BPA and BPA analogs (BPC, DPA, DES) at a concentration of 5 ng/mL.

acid (DPA), and Diethylstilbestrol (DES) were tested at a concentration of 5 ng/mL. As shown in Figure 5, the CD signals at 533 nm for BPC, DPA, and DES showed no obvious variation compared with the control without targets, which demonstrated that the three analogs did not bind with the BPA aptamer and the assembled dimers were not separated into single nanoparticles. These results showed that the BPA aptamer has highly selective for BPA but not the other BPA analogs. Thus, the aptamer-based sensor for detecting BPA was superior to the antibody.

The reliability of this sensor in practical applications was evaluated by performing a recovery test in tap water. Tap water was spiked with different concentrations of BPA standard samples, 0.05, 0.1, 0.5, and 5 ng/mL. The results are shown in Table 2, and the recovery was in the range 93%−98.4%.These satisfactory results indicated that this sensor was feasible for the analysis of real samples.

Table 2. Determination of BPA Spiked into Tap Water

sample	spiked concentration (ng mL^{-1})	detected concentration mean^{a} ± SD^{b} (ng mL^{-1})	recovery (%)
water	0.05	0.047 ± 0.002	94
	0.1	0.093 ± 0.007	93
	0.5	0.486 ± 0.016	97.2
	1	0.96 ± 0.047	96
	5	4.92 ± 0.214	98.4

^{a}The mean of five experiments. ^{b}SD = standard deviation.

4. CONCLUSIONS

In summary, based on the assembled asymmetric dimers using the BPA aptamer and its complementary sequence, a sensitive

Table 1. Comparison of This Work with Other Methods for Detecting BPA Based on Plasmonic Nanoparticles

detection method	recognizing unit	limit of detection	detection range	ref
resonance Rayleigh scattering	aptamer	83 pg/mL	3.33−333.3 ng/mL	46
colorimetric method based on Au NP aggregates fluorescence quench	aptamer	0.1 ng/mL	1−10 000 ng/mL	25
		0.01 pg/mL	0.1−10 000 pg/mL	
aptamer lateral flow strip using Au NP aggregation	aptamer	76 pg/mL	0.05−10 ng/mL	47
immunochromatographic lateral flow using Au NP aggregation	antibody/antigen	5 ng/mL		48
colorimetric method based on Au NP aggregates	aptamer	49 pg/mL	0.01−100 ng/mL	49
Au NP immunosensor	antibody/antigen	20 pg/mL	0.05−10 ng/mL	38
surface enhanced Raman scattering-based Ag NP		∼0.1 ng/mL		50
plasmonic chiral aptasensor	aptamer	8 pg/mL	0.02−5 ng/mL	this work

dx.doi.org/10.1021/am4043678 | ACS Appl. Mater. Interfaces 2014, 6, 364−369

plasmonic chirality-based sensor was developed using the CD signal as an indicator. The intensity of the CD signal depended on the number of asymmetric dimers, which corresponded to the concentration of BPA. Under optimized conditions, a LOD of 0.008 ng/mL was obtained in the range 0.02−5 ng/mL. This aptamer-based method has greater specificity than the immunorecognition-based method and showed no cross-reaction with BPA analogs. This sensor was highly sensitive, specific, and had a low LOD for detecting and quantifying BPA. Importantly, this method can also be used for the analysis of real samples with excellent recovery.

■ ASSOCIATED CONTENT

Supporting Information

Additional experimental details. Figures showing standard linear curve of the PL intensity at 518 nm with the variation FAM-DNA concentration, CD spectra of Au NPs symmetric and asymmetric dimers, and statistical analysis of the number of Au NPs in the assembled samples. This material is available free of charge via the Internet at http://pubs.acs.org.

■ AUTHOR INFORMATION

Corresponding Author

* H. Kuang. E-mail: kuangh@jiangnan.edu.cn.

Author Contributions

†These authors contributed to this paper equally.

Notes

The authors declare no competing financial interest.

■ ACKNOWLEDGMENTS

This work is financially supported by the National Natural Science Foundation of China (21071066, 91027038, 21101079, 21175034, 21371081, 21301073), the Key Programs from MOST (2012BAC01B07, 2012AA06A303, 2012BAD29B04, 2012BAK11B01, 2011BAK10B07, 2011BAK10B01, 2010AA06Z302, 2010DFB3047, 2013ZX08012-001, 2012BAK17B10, 2012BAK08B01, 2012YQ090194, 2012BAD29B05, 2013AA065501), and grants from Jiangsu Province, MOF and MOE (NCET-12-0879, BE2011626, BE2013613, BE2013611, 201310128, 201210127, 201210036, 201310135, 311002, JUSRP51308A).

■ REFERENCES

(1) Liao, C.; Kannan, K. *Environ. Sci. Technol.* **2011**, *45*, 6761−6768.
(2) Schwartz, A. W.; Landrigan, P. J. *Environ. Health Perspect.* **2012**, *120*, a14−A15.
(3) Fromme, H.; Küchler, T.; Otto, T.; Pilz, K.; Müller, J.; Wenzel, A. *Water Res.* **2002**, *36*, 1429−1438.
(4) Boyd, G. R.; Palmeri, J. M.; Zhang, S.; Grimm, D. A. *Sci. Total Environ.* **2004**, *333*, 137−148.
(5) Vandenberg, L. N.; Maffini, M. V.; Sonnenschein, C.; Rubin, B. S.; Soto, A. M. *Endocr. Rev.* **2009**, *30*, 75−95.
(6) Lee, H. J.; Chattopadhyay, S.; Gong, E. Y.; Ahn, R. S.; Lee, K. *Toxicol. Sci.* **2003**, *75*, 40−46.
(7) Rubin, B. S. *J. Steroid Biochem.* **2011**, *127*, 27−34.
(8) Bouskine, A.; Nebout, M.; Brücker-Davis, F.; Benahmed, M.; Fenichel, P. *Environ. Health. Perspect.* **2009**, *117*, 1053−1058.
(9) Yoon, Y.; Westerhoff, P.; Snyder, S. A.; Esparza, M. *Water Res.* **2003**, *37*, 3530−3537.
(10) Shao, B.; Han, H.; Hu, J.; Zhao, J.; Wu, G.; Xue, Y.; Ma, Y.; Zhang, S. *Anal. Chim. Acta* **2005**, *530*, 245−252.
(11) Tominaga, T.; Negishi, T.; Hirooka, H.; Miyachi, A.; Inoue, A.; Hayasaka, I.; Yoshikawa, Y. *Toxicology* **2006**, *226*, 208−217.
(12) Li, D.; Park, J.; Oh, J.-R. *Anal. Chem.* **2001**, *73*, 3089−3095.
(13) Fukata, H.; Miyagawa, H.; Yamazaki, N.; Mori, C. *Toxicol. Mech. Methods* **2006**, *16*, 427−430.
(14) Sajiki, J.; Hasegawa, Y.; Hashimoto, H.; Makabe, Y.; Miyamoto, F.; Yanagibori, R.; Shin, J.; Shimidzu, Y.; Morigami, T. *Toxicol. Mech. Methods* **2008**, *18*, 733−738.
(15) Willner, I.; Zayats, M. *Angew. Chem., Int. Ed.* **2007**, *46*, 6408−6418.
(16) Song, S.; Wang, L.; Li, J.; Fan, C.; Zhao, J. *TrAC, Trends Anal. Chem.* **2008**, *27*, 108−117.
(17) McCauley, T. G.; Hamaguchi, N.; Stanton, M. *Anal. Biochem.* **2003**, *319*, 244−250.
(18) Syed, M. A.; Pervaiz, S. *Oligonucleotides* **2010**, *20*, 215−224.
(19) Liu, J. W.; Lu, Y. *Angew. Chem., Int. Ed.* **2006**, *45*, 90−94.
(20) Liu, J. *Phys. Chem. Chem. Phys.* **2012**, *14*, 10485−10496.
(21) Jo, M.; Ahn, J.-Y.; Lee, J.; Lee, S.; Hong, S. W.; Yoo, J.-W.; Kang, J.; Dua, P.; Lee, D.-K.; Hong, S. *Oligonucleotides* **2011**, *21*, 85−91.
(22) Lee, J.; Jo, M.; Kim, T. H.; Ahn, J.-Y.; Lee, D.-K.; Kim, S.; Hong, S. *Lab Chip* **2011**, *11*, 52−56.
(23) Mei, Z.; Chu, H.; Chen, W.; Xue, F.; Liu, J.; Xu, H.; Zhang, R.; Zheng, L. *Biosens. Bioelectron.* **2013**, *39*, 26−30.
(24) Xue, F.; Wu, J.; Chu, H.; Mei, Z.; Ye, Y.; Liu, J.; Zhang, R.; Peng, C.; Zheng, L.; Chen, W. *Microchim. Acta* **2013**, *180*, 109−115.
(25) Vasanth, K.; SelvaKumar, S. L.; Thakur, M. S. *Chem. Commun.* **2013**, *49*, 5960−5962.
(26) Huang, J.; Zhang, X.; Liu, S.; Lin, Q.; He, X.; Xing, X.; Lian, W. *J. Appl. Electrochem.* **2011**, *41*, 1323−1328.
(27) Ray, P. C. *Chem. Rev.* **2010**, *110*, 5332−5365.
(28) Liu, J.; Son, Y.-C.; Cai, J.; Shen, X.; Suib, S. L.; Aindow, M. *Chem. Mater.* **2004**, *16*, 276−285.
(29) Guo, L.; Xu, Y.; Ferhan, A.; Chen, G.; Kim, D. *J. Am. Chem. Soc.* **2013**, *135*, 12338−12345.
(30) Xia, Y.; Zhou, Y.; Tang, Z. *Nanoscale* **2011**, *3*, 1374−1382.
(31) Sheikholeslami, S.; Jun, Y. W.; Jain, P. K.; Alivisatos, A. P. *Nano Lett.* **2010**, *10*, 2655−2660.
(32) Kuzyk, A.; Schreiber, R.; Fan, Z.; Pardatscher, G.; Roller, E.-M.; Högele, A.; Simmel, F. C.; Govorov, A. O.; Liedl, T. *Nature* **2012**, *483*, 311−314.
(33) Mastroianni, A.; Claridge, S.; Alivisatos, A. P. *J. Am. Chem. Soc.* **2009**, *131*, 8455−8459.
(34) Li, Z.; Zhu, Z.; Liu, W.; Zhou, Y.; Han, B.; Gao, Y.; Tang, Z. *J. Am. Chem. Soc.* **2012**, *134*, 3322−3325.
(35) Lan, X.; Chen, Z.; Dai, G.; Lu, X.; Ni, W.; Wang, Q. *J. Am. Chem. Soc.* **2013**, *135*, 11441−11444.
(36) Zhao, Y.; Xu, L.; Kuang, H.; Wang, L.; Xu, C. *J. Mater. Chem.* **2012**, *22*, 5574−5580.
(37) Zhao, Y.; Xu, L.; Liz-Marzán, L. M.; Kuang, H.; Ma, W.; Garcia de Abajo, J.; Kotov, N. A.; Wang, L.; Xu, C. *J. Phys. Chem. Lett.* **2013**, *4*, 641−647.
(38) Kuang, H.; Ma, W.; Xu, L.; Wang, L.; Xu, C. *Acc. Chem. Res.* **2013**, DOI: 10.1021/ar300206m.
(39) Zhu, Y.; Xu, L.; Ma, W.; Xu, Z.; Kuang, H.; Wang, L.; Xu, C. *Chem. Commun.* **2012**, *48*, 11889−11891.
(40) Xu, Z.; Xu, L.; Zhu, Y.; Ma, W.; Kuang, H.; Wang, L.; Xu, C. *Chem. Commun.* **2012**, *48*, 5760−5762.
(41) Liu, X.; Dai, Q.; Austin, L.; Coutts, J.; Knowles, G.; Zou, J. H.; Chen, H.; Huo, Q. *J. Am. Chem. Soc.* **2008**, *130*, 2780−2782.
(42) Xu, L. G.; Kuang, H.; Xu, C. L.; Ma, W.; Wang, L. B.; Kotov, N. A. *J. Am. Chem. Soc.* **2012**, *134*, 1699−1709.
(43) Linette, M. D.; Chad, A. M.; Robert, C. M.; Robert, A. R.; Robert, L. L.; Robert, E.; Viswanadham., G. *Anal. Chem.* **2000**, *72*, 5535−5541.
(44) Zhu, Y. Y.; Xu, L. G.; Ma, W.; Chen, W.; Yan, W. J.; Kuang, H.; Wang, L. B.; Xu, C. L. *Biosens. Bioelectron.* **2011**, *26*, 4393−4398.
(45) Billaud, P.; Marhaba, S.; Cottancin, E.; Arnaud, L.; Bachelier, G.; Bonnet, C.; Del Fatti, N.; Lermé, J.; Vallée, F.; Vialle, J.-L. *J. Phys. Chem. C* **2008**, *112*, 978−982.
(46) Sonnichsen, C.; Reinhard, B. M.; Liphardt, J.; Alivisatos, A. P. *Nat. Biotechnol.* **2005**, *23*, 741−745.

(47) Reinhard, B. M.; Siu, M.; Agarwal, H.; Alivisatos, A. P.; Liphardt, J. *Nano Lett.* **2005**, *5*, 2246−2252.
(48) Yao, D. M.; Wen, G. Q.; Jiang, Z. L. *RSC Adv.* **2013**, *3*, 13353−13356.
(49) Mei, Z. L.; Qu, W.; Deng, Y.; Chu, H. Q.; Cao, J. X.; Xue, F.; Zheng, L.; El-Nezamic, H. S.; Wu, Y. C.; Chen, W. *Biosens. Bioelectron.* **2013**, *49*, 457−461.
(50) Mei, Z. L.; Deng, Y.; Chu, H. Q.; Xue, F.; Zhong, Y. H.; Wu, J. J.; Yang, H.; Wang, Z. C.; Zheng, L.; Chen, W. *Microchim. Acta* **2013**, *180*, 279−285.
(51) Mei, Z. L.; Chu, H. Q.; Chen, W.; Xue, F.; Liu, J.; Xu, H. N.; Zhang, R.; Zheng, L. *Biosens. Bioelectron.* **2013**, *39*, 26−30.
(52) Han, X. X.; Pienpinijtham, P.; Zhao, B.; Ozaki, Y. *Anal. Chem.* **2011**, *83*, 8582−8588.
(53) Thomas, S. W.; Joly, G. D.; Swager, T. M. *Chem. Rev.* **2007**, *107*, 1339−1386.
(54) Kobayashi, H.; Ogawa, M.; Alford, R.; Choyke, P. L.; Urano, Y. *Chem. Rev.* **2010**, *110*, 2620−2640.
(55) Kolpashchikov, D. M. *Chem. Rev.* **2010**, *110*, 4709−4723.